Stem Cell Reports
Article
OPEN ACCESS

Combined KIT and FGFR2b Signaling Regulates Epithelial Progenitor Expansion during Organogenesis

Isabelle M.A. Lombaert,[1] Shaun R. Abrams,[1] Li Li,[3] Veraragavan P. Eswarakumar,[3] Aditya J. Sethi,[2] Robert L. Witt,[4] and Matthew P. Hoffman[1,*]
[1]Matrix and Morphogenesis Section, Laboratory of Cell and Developmental Biology
[2]Developmental Mechanisms Section
National Institute of Dental and Craniofacial Research, National Institutes of Health, Bethesda, MD 20892, USA
[3]Department of Orthopedics & Rehabilitation, Yale University School of Medicine, New Haven, CT 06520, USA
[4]Head & Neck Multidisciplinary Clinic, Helen F. Graham Cancer Center of Christiana Care, Newark, DE 19713, USA
*Correspondence: mhoffman@mail.nih.gov
http://dx.doi.org/10.1016/j.stemcr.2013.10.013

SUMMARY

Organ formation and regeneration require epithelial progenitor expansion to engineer, maintain, and repair the branched tissue architecture. Identifying the mechanisms that control progenitor expansion will inform therapeutic organ (re)generation. Here, we discover that combined KIT and fibroblast growth factor receptor 2b (FGFR2b) signaling specifically increases distal progenitor expansion during salivary gland organogenesis. FGFR2b signaling upregulates the epithelial KIT pathway so that combined KIT/FGFR2b signaling, via separate AKT and mitogen-activated protein kinase (MAPK) pathways, amplifies FGFR2b-dependent transcription. Combined KIT/FGFR2b signaling selectively expands the number of KIT+K14+SOX10+ distal progenitors, and a genetic loss of KIT signaling depletes the distal progenitors but also unexpectedly depletes the K5+ proximal progenitors. This occurs because the distal progenitors produce neurotrophic factors that support gland innervation, which maintains the proximal progenitors. Furthermore, a rare population of KIT+FGFR2b+ cells is present in adult glands, in which KIT signaling also regulates epithelial-neuronal communication during homeostasis. Our findings provide a framework to direct regeneration of branched epithelial organs.

INTRODUCTION

During organogenesis, epithelial progenitor cells generate the branched architecture of the tissue. These progenitors must increase in number while retaining their progenitor qualities, in a process known as expansion. Organogenesis further involves communication between expanding progenitors and other cell types located in the niche or local microenvironment (Wagers, 2012). Stromal, endothelial, and neuronal cells provide external cues that control the number of progenitors and their survival, maintenance, and differentiation (Kiger et al., 2000; Knox et al., 2010; Shen et al., 2004). Thus, it is imperative to understand the mechanisms by which progenitors expand and how they communicate with other cell types in order to regenerate or reengineer the branched architecture of epithelial organs.

KIT (C-KIT, CD117), a receptor tyrosine kinase (RTK), has been studied extensively in hematopoietic progenitors (Kent et al., 2008), but less is known about its function in epithelial progenitors. The ligand for KIT is stem cell factor (SCF), the gene product of *Kitl*. KIT signals via numerous pathways, including phosphatidylinositol 3-kinase (PI3K), phospholipase C γ (PLCγ), mitogen-activated protein kinase (MAPK), and Janus kinase/Signal Transducer and Activator of Transcription (JAK/STAT) (Lemmon and Schlessinger, 2010), and can transactivate other receptors (Jahn et al., 2007; Wu et al., 1995). Importantly, KIT-expressing (KIT+) progenitors form and regenerate various epithelial organs. Prostate tissue can be generated from a single KIT+ cell (Leong et al., 2008), epithelial-specific KIT+ progenitors functionally regenerate irradiated salivary glands (Lombaert et al., 2008; Nanduri et al., 2013), and KIT+ cells repair lungs postthoracotomy (Kajstura et al., 2011). These findings suggest that epithelial KIT+ progenitors somehow lay the foundation for branching organ architecture. Importantly, the loss of KIT signaling due to a homozygous SNP (Chabot et al., 1988), $Kit^{W/W}$, is lethal by embryonic day 14 (E14) due to hematopoietic defects, but the effects of this mutation on epithelial progenitors and organogenesis are unclear.

Severe defects in epithelial organogenesis occur in mice lacking *Fgf10* or its receptor, *Fgfr2b*, and provide valuable insight into epithelial progenitor cell biology. Many organs, such as the salivary glands and lungs, do not form or are hypoplastic (De Moerlooze et al., 2000; Ohuchi et al., 2000). These phenotypes suggest defects in the survival, maintenance, and/or expansion of epithelial progenitors. In addition, mutations in fibroblast growth factor receptor 2 (FGFR2) and KIT occur in many epithelial tumors, and both receptors are being targeted with specific RTK inhibitors in breast, lung, liver, salivary gland, skin, renal, gastrointestinal, colorectal, ovarian, and uterine cancers (Casaletto and McClatchey, 2012; Hanahan and Weinberg, 2011; Lemmon and Schlessinger, 2010; Takeuchi and Ito, 2011). We thus hypothesized that an interaction

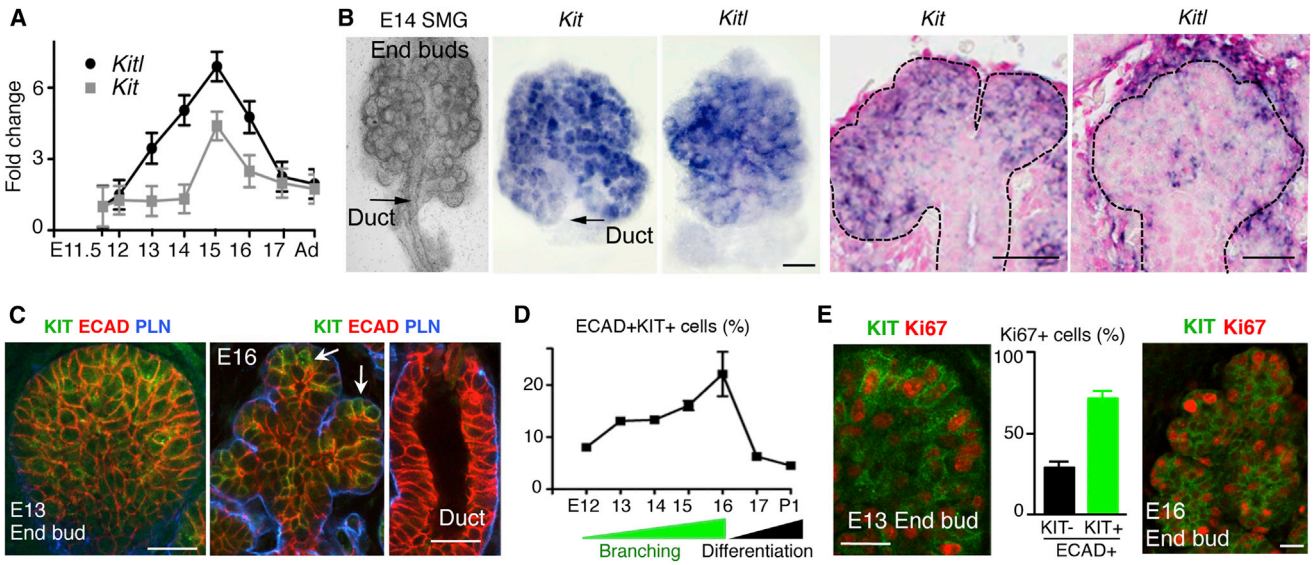

Figure 1. *Kit* and *Kitl* Increase during Branching Morphogenesis, and KIT+ Progenitor Expansion Occurs in Endbuds

(A) qPCR analysis of *Kit* and *Kitl* mRNA expression during SMG development. Mean ± SEM, n > 3 biological SMGs at each developmental stage. Data were normalized to *Rps29* and E11.5 SMG.

(B) E14 SMGs. Whole-mount in situ analysis of *Kit* and *Kitl* mRNA expression, sections stained with Nuclear Fast Red. Black dashed lines outline epithelia. Scale bars, 200 μm for whole mounts and 25 μm for sections.

(C) Staining of E13 and E16 SMGs for KIT, ECAD, and basement membrane (Perlecan [PLN]). Images are 1 μm confocal sections. Arrow indicates endbuds. Scale bars, 20 μm.

(D) FACS analysis (% of cells/SMG) of ECAD+KIT+ cells during development. Data are mean ± SEM, n > 3 biological independent samples at each developmental stage.

(E) KIT and Ki67 staining of E13 and E16 SMG endbuds. FACS analysis of E13 SMG showing the percentage of proliferating cells (Ki67+) in KIT− or KIT+ cells. Scale bar, 20 μm; n > 3 biological samples.

See also Figure S1.

between FGFR2b and KIT signaling could regulate epithelial progenitor expansion during organogenesis.

To investigate this hypothesis, we studied mouse submandibular glands (SMGs), which develop by reiterative rounds of distal endbud and proximal duct formation, and require communication with the neuronal niche (Knox et al., 2010). We discovered that FGFR2b signaling upregulates the epithelial KIT pathway so that combined KIT/FGFR2b signaling, via separate AKT and MAPK pathways, amplifies FGFR2b-dependent transcription. The combined KIT and FGFR2b signaling increases the number of KIT+FGFR2b+ distal progenitors, but loss of KIT signaling depletes these progenitors. This KIT/FGFR2b-dependent mechanism is conserved during adult tissue homeostasis and in other branching organs.

RESULTS

KIT+ Progenitor Expansion Occurs in Endbuds during SMG Branching Morphogenesis

We first investigated the developmental expression and localization of *Kit* and *Kitl* mRNA by quantitative PCR (qPCR; Figure 1A), in situ hybridization (Figure 1B), and microarray during development (Figure S1A available online). mRNA products of both *Kit* and *Kitl* were detectable during gland initiation at E11.5, when the initial endbud forms distal to a primary duct, and expression of both peaked at ~E15 (Figure 1A). From E12 to E15, branching morphogenesis occurred with reiterative rounds of distal endbud expansion and proximal duct formation. Whereas *Kit* mRNA was localized to endbuds, *Kitl* mRNA was found mainly in the mesenchyme around the endbuds, but was also detected within endbuds (Figure 1B), as confirmed by qPCR analysis of isolated E13 endbuds, ducts, and mesenchyme (Figure S1B). During branching morphogenesis, KIT protein was localized to E-cadherin+ (ECAD+) endbud cells (Figure 1C, E16, arrows), but was not detected in ducts (KIT−) (Figures 1B and 1C). Fluorescence-activated cell sorting (FACS) analysis confirmed that during the rapid branching phase, the number of epithelial KIT+ cells (ECAD+KIT+) increased from 10% to 20% of total cells in the intact SMG (Figures 1D and S1C). Furthermore, FACS analysis and Ki67 staining showed that E13 ECAD+KIT+ cells were highly proliferative (Figure 1E), since ~70% of cycling SMG cells (Ki67+) were KIT+. This highly

proliferative state occurred up to E16 (Figure 1E). By the time secretory differentiation began after E16, both *Kit* and *Kitl* mRNA expression decreased (Figures 1A and S1A). KIT+ cells accounted for only ~3% of total cells at postnatal day 1 (P1; Figure 1D), which is comparable to levels in adult SMGs (Lombaert et al., 2008). Since the number of KIT+ endbud cells increases during branching morphogenesis, the data suggest that KIT+ progenitor expansion occurs in endbuds.

FGFR2b Signaling Upregulates an Autocrine Epithelial KIT Pathway

FGFR2b signaling is essential for the survival and proliferation of epithelial endbuds; however, it is unclear whether it regulates progenitor expansion. Since KIT marks the endbud progenitors, we hypothesized that FGFR2b signaling controls KIT+ progenitor expansion by regulating KIT function. We tested this by culturing isolated SMG epithelia for 2 hr with inhibitors of FGFR (SU5402 [SU]), MAPK (UO126), PI3K (LY29052) and PLCγ (U7312), and FGFR2b ligands and measuring downstream gene expression. *Kitl* was rapidly downregulated with SU or UO126 (Figure 2A). In contrast, addition of the FGFR2b ligands FGF1, FGF7, and FGF10 specifically upregulated *Kitl* (Figure 2B), whereas other factors, such as FGF2, FGF8b, BMP2, BMP4, BMP7, insulin growth factor 2 (IGF2), transforming growth factor β1 (TGFβ1), TGFβ2, carbachol (CCh), heparin-binding EGF-like growth factor (HBEGF), and SCF, did not. In addition, *Kit* was upregulated 6 hr after FGF10 addition (Figure 2C). Thus, FGFR2b signaling positively regulates *Kitl* expression in the epithelium, which may result in an autocrine activation of KIT in the endbud progenitors by epithelial SCF.

FGFR2b and KIT Signal via Separate MAPK and AKT Pathways

Because FGFR2b signaling may upregulate an autocrine epithelial KIT pathway, we investigated the molecular interactions of these pathways and paracrine KIT signaling using cell lines expressing KIT and FGFR2b, and isolated SMG epithelium. We were unable to coimmunoprecipitate FGFR2b and KIT from SMG epithelium (not shown). Since we could not show a direct interaction, we investigated possible transactivation or signaling crosstalk on two levels. First, at the ligand level, we used a rat myoblast cell line (L6) expressing either Flag-tagged FGFR2b (FGFR2b-FL) or hemagglutinin (HA)-tagged KIT (KIT-HA) to show that the ligands are specific and do not phosphorylate (Anti-PY) the other receptor in these cells (Figure 2D). Second, at the receptor level, we used L6 cells expressing both receptors (KIT+FGFR2b+L6) to show that KIT and FGFR2b do not transactivate (Anti-PY) each other (Figure 2E). We then used FGFR2b+L6 or KIT+L6 cells to show that pERK1/2 is downstream of both KIT and FGFR2b, and that the KIT inhibitor ISCK03 (ISCK) specifically reduced SCF/KIT-dependent pERK1/2, whereas SU specifically reduced pERK12 downstream of FGF10/FGFR2b (Figure 2F). We confirmed that ISCK specifically inhibited KIT, but not FGFR2b, phosphorylation (Figure S2A). Further, we used a KIT+ human leukemic cell line, Mo7e, which does not express FGFR2b, to confirm that SU did not inhibit SCF-dependent pKIT^{Y721} and downstream pAKT, whereas ISCK did (Figure S2B). Neither inhibitor reduced pERK1/2, which is downstream of other RTKs in Mo7e cells. Taken together, these data suggest that FGFR2b and KIT do not transactivate each other, and that separate MAPK and AKT signaling pathways occur downstream of each receptor.

We also measured phosphorylation of KIT^{Y721} in isolated SMG epithelia cultured for 24 hr with FGF10 and then treated for 15 min with additional SCF or FGF10 and/or SU and ISCK. There was a robust baseline level of pKIT^{Y721}, and SCF further increased pKIT^{Y721} and pAKT, whereas FGF10 increased pERK1/2 (Figure 2G). As expected, SU reduced pERK1/2 downstream of FGF10, and ISCK reduced pAKT downstream of SCF. Exogenous FGF10 also increased pKIT^{Y721}, which is likely due to endogenous epithelial SCF (i.e., autocrine KIT signaling in the epithelium) being enhanced by FGF10. This FGF10-dependent pKIT^{Y721} and pAKT were reduced by SU or SU+ISCK, suggesting that in SMG epithelia, FGF10 may transactivate KIT or that SU inhibits another receptor that transactivates KIT. We also show that ISCK reduced pKIT^{Y721} and pAKT to near control levels after SCF treatment and partially reduced pKIT^{Y721} after FGF10 treatment. In other experiments, ISCK was specific and did not reduce pERK1/2 or pAKT downstream of FGFR2b (with FGF10), epidermal growth factor receptor (EGFR; with HBEGF), or FGFR1 receptors (with FGF2) after 1 hr (Figures S2C and S2D). These data suggest that separate KIT and FGFR2b signaling occurs in SMG epithelia KIT+ progenitors.

Combined FGFR2b and KIT Signaling Amplifies FGFR2b-Dependent Transcription

To investigate how separate KIT and FGFR2b signaling pathways regulate progenitor expansion, we treated isolated SMG epithelia with SCF and FGF10 alone or in combination. The downstream phosphorylation with SCF and FGF10 was additive and led to enhanced and sustained phosphorylation of SHP2, AKT, and ERK1/2 compared with either SCF or FGF10 alone (Figure 3A). We predicted that this might increase downstream gene transcription. Thus, we measured the expression of a cassette of transcription factors (TFs), *Sox10*, *Myc*, *Etv4*, *Etv5*, and *ΔNp63*, all of which are expressed in endbuds and potentially involved in SMG progenitor expansion (Lombaert et al., 2011).

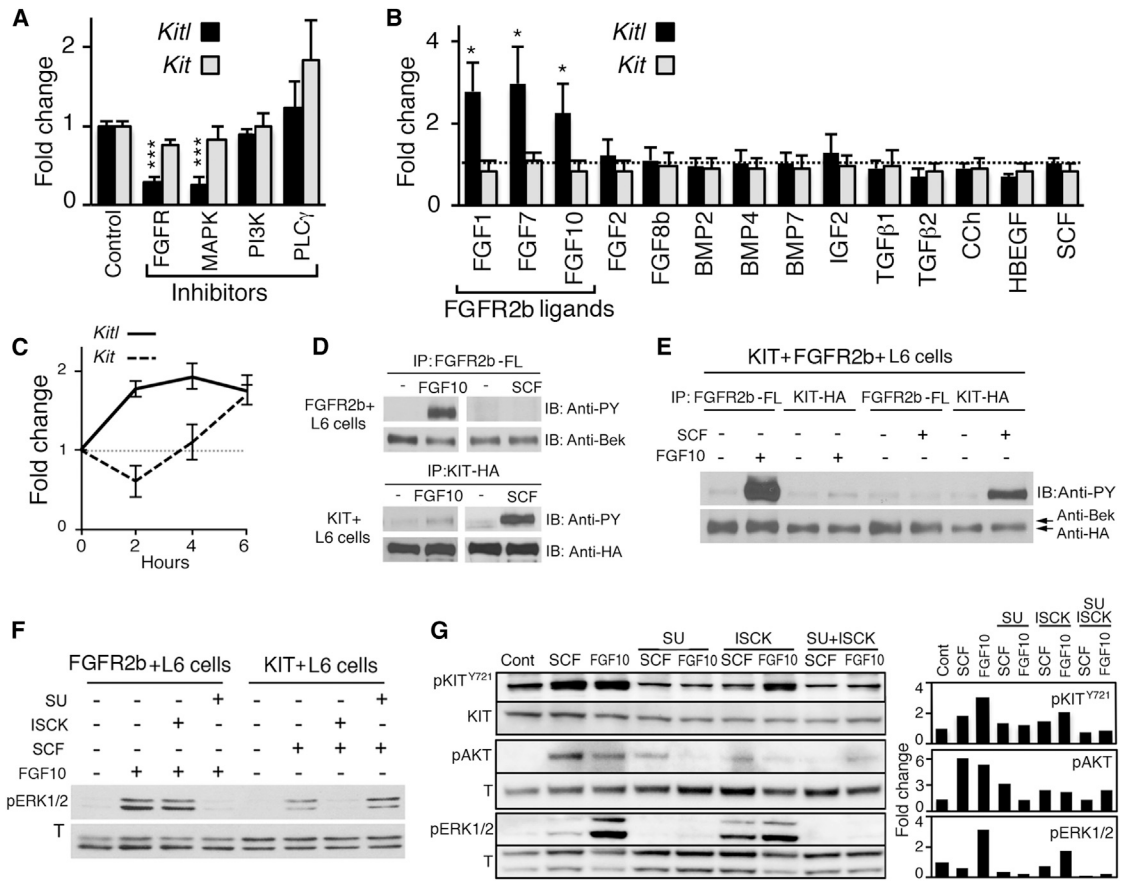

Figure 2. FGFR2b Signaling Upregulates the Autocrine Epithelial KIT Pathway, and the Receptors Signal via Separate MAPK and AKT Pathways

(A) qPCR analysis of *Kitl* and *Kit* in E13 epithelia 2 hr after addition of FGF10 and inhibitors: Control (DMSO), FGFR (SU5402), MAPK (U0126), PI3K (LY29052), and PLCγ (U7312). Data are mean ± SEM, normalized to *Rsp29* and Control. One-way ANOVA with post-hoc Dunnett's test; ***$p < 0.001$, n = 3 biological samples.

(B) qPCR analysis of E13 epithelia 2 hr after growth factor addition. Data are mean ± SEM, normalized to *Rsp29* and epithelia at 0 hr (dashed line). Unpaired t test; *$p < 0.05$, n = 3 biological samples.

(C) qPCR analysis of E13 epithelia at different times after FGF10 treatment. Data are mean ± SEM, normalized to *Rsp29* and 0 hr (gray dashed line), n = 3 biological samples.

(D) Immunoblot for p-tyrosine kinase (PY), FGFR2 (Anti-Bek), and KIT (Anti-HA) after immunoprecipitation (IP) of FGFR2b-FL- or KIT-HA-tagged proteins from FGFR2b+L6 or KIT+L6 cells 15 min after growth factor stimulation with either FGF10 or SCF.

(E) Immunoblot of phosphotyrosine (PY) and FGFR2 (Bek), and KIT (HA) after IP of Flag-FGFR2b or HA-KIT in KIT+FGFR2b+ L6 cells, after FGF10, SCF, and/or ISCK treatment.

(F) Immunoblot of pERK1/2 and total (T) ERK after FGFR2b+L6 or KIT+L6 cells were treated with FGF10, SCF, SU, and ISCK.

(G) Immunoblot of $pKIT^{Y721}$, pAKT, pERK1/2, and total (T) AKT or ERK1/2 and KIT after epithelia were cultured for 5 min with SCF and/or FGF10 in the presence of ISCK or SU. Representative blot, n = 3 biological samples.

See also Figure S2.

Costimulation with FGF10+SCF for 3 hr increased expression of *Sox10*, *Myc*, *Etv4*, and *Etv5*, but not *ΔNp63*, above the level observed with FGF10 alone (Figure 3B). We show that KIT signaling was essential for this increased expression, since ISCK reduced expression to a level similar to that obtained with FGF10 alone. The PI3K inhibitor LY29052 (which reduces pAKT), but not the PLCγ inhibitor U73122, mimicked this effect, suggesting that the positive regulation by KIT occurs via increased PI3K/AKT signaling. We confirmed that activation of FGFR2b signaling upregulated TFs in a MAPK-dependent manner (Figure S3). Importantly, SCF alone did not have direct effects on TF gene expression. Furthermore, KIT and FGFR2b regulate these conserved TF targets in cells that do not

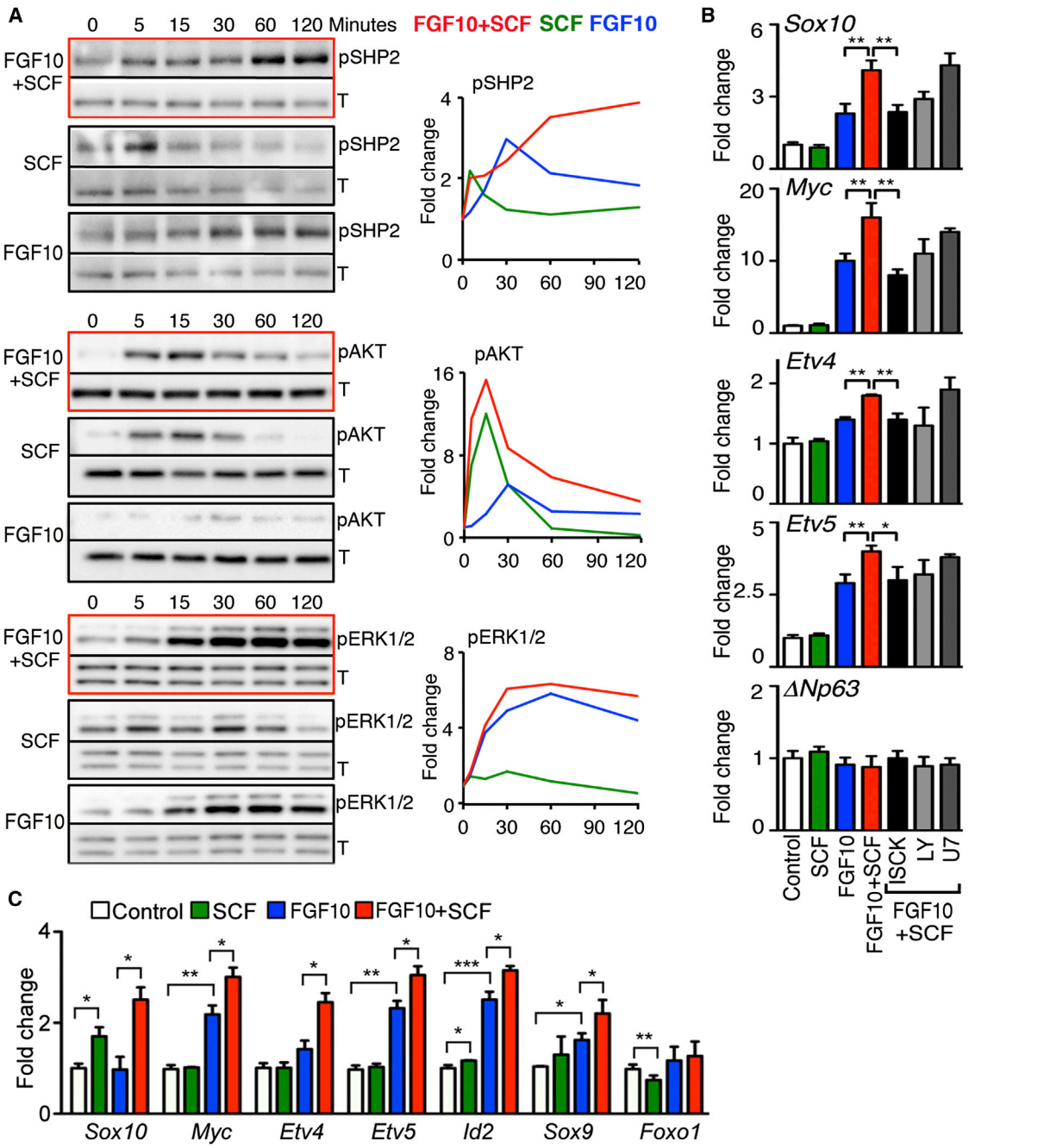

Figure 3. KIT Signaling Increases Expression of FGFR2b-Dependent Transcriptional Targets

(A) Immunoblot of pSHP2, pAKT, pERK1/2, and total (T) SHP2, AKT, or ERK1/2 at different time points after addition of SCF and/or FGF10. Graphs represent quantification of a representative blot, n = 3 biological samples.

(B and C) qPCR analysis of gene expression in SMG epithelia (B) or KIT+FGFR2b+L6 cells (C) cultured for 3 hr with SCF and/or FGF10. SMG epithelia were treated with inhibitors ISCK, LY29052 (LY), or U73122 (U7). Unpaired t test; *p < 0.05, **p < 0.01. Statistics compare FGF10+SCF with FGF10 alone or with FGF10+SCF+ISCK; n = 3 biological samples.

See also Figure S3.

endogenously express the receptors, as was observed with KIT+FGFR2b+L6 cells stimulated with SCF/FGF10 (Figure 3C). We conclude that the KIT and FGFR2b signaling pathways converge to increase expression of a conserved cassette of FGFR2b-dependent TFs during the expansion of KIT+ endbud progenitors.

Endbuds Contain Distinct Populations of KIT+K14+ Distal and KIT+K5+ Proximal Progenitors

In addition to KIT+ endbud progenitors, we previously identified K5-expressing (K5+) progenitors that are essential for proximal K19+ duct development (Knox et al., 2010). Therefore, we characterized the distinct cell types within the KIT+ population by their keratin (K) expression. Usually, K5 pairs with K14 (Rock et al., 2009), but in SMG KIT+ endbuds the basal K14+ cells did not coexpress K5 (Figure 4A). This unexpected observation led us to characterize the progenitor potential of K14+ cells by genetic lineage tracing. We labeled K14+ cells and their progeny with GFP using a K14Cre mouse crossed with a $Rosa^{mTmG}$ reporter strain. At P1, we observed GFP expression in ECAD+ epithelial cells (Figures 4B, S4A, and S4B). The K14+ progenitors are multipotent, as their progeny included K5+ ductal cells, Amylase-producing acinar cells, and smooth-muscle-Actin+ myoepithelial cells (Figure S4C). FACS analysis showed that KIT+K8+ epithelial endbud cells are a heterogeneous population of distal K14+ (14% ± 3%) and proximal K5+ progenitors (10% ± 2%; Figure 4C). Furthermore, proximal K5+ progenitors and their progeny (K5+K19+ and K19+ cells) were localized centrally in endbuds and were contiguous with the duct (Figure 4A). KIT+K8+ cells (56% ± 4%) that did not express K14, K5, or K19 were located between the basal layer and central duct cells of the endbud (Figure 4A). We conclude that the endbud contains two distinct populations of progenitors: a pool of distal KIT+K14+ progenitors and a pool of proximal KIT+K5+ progenitors.

KIT and FGFR2b Signaling Selectively Expands Distal Progenitors in the Endbud

Next, we investigated whether KIT and FGFR2b regulate the expansion of both distal KIT+K14+ and proximal KIT+K5+ progenitors. Combined FGF10+SCF treatment increased K14 expression in isolated epithelial endbuds within 24 hr (Figure 4D). Staining for KIT, SOX10, and p63 confirmed that multiple cell layers of K14+ progenitors were present in the endbud. Conversely, central K19+ ductal cells were reduced as compared with FGF10 treatment alone. Consistent with this, *Krt14* and *Sox10* increased, whereas *Krt19* decreased, with FGF10+SCF versus FGF10 treatment (Figure S4D). To confirm that KIT and FGFR2b signaling selectively amplify KIT+K14+ distal progenitors, we cultured E13 SMGs with FGF10−/+ SCF and did a FACS analysis. Similar to the case with isolated epithelium, combined KIT and FGFR2b signaling expanded the number of K14+, KIT+, and SOX10+ cells (Figures 4E and S4E). The KIT+K14+ distal progenitors increased in number at the expense of KIT+K14− cells (Figure 4F). This is reflected in the doubling number of all KIT+K14+ cells, including those coexpressing K5 and/or K19: K14+ (K14+K5−K19−), K14+K5+ (K14+K5+K19−), K14+K19+ (K14+K5−K19+), and K14+K5+K19+. Immunostaining validated the FACS data, showing that endbuds contained more cells expressing K14, SOX10, and KIT (Figure 4G). Thus, KIT and FGFR2b selectively expand distal KIT+K14+ progenitors, but not proximal KIT+K5+ progenitors or their K19+ progeny. We also measured proliferation in intact SMGs and isolated epithelia after FGF10−/+ SCF stimulation. FACS analyses showed that the number of proliferating (Ki67+) and epithelial (ECAD+) SMG cells did not change with FGF10+SCF treatments (Figure 4E), and there was no difference in gland morphology or endbud number (Figure S4F). In isolated epithelia, SCF alone did not support survival or proliferation (Figures S4G and S4H). Since KIT signaling alone did not affect proliferation, we conclude that selective expansion of KIT+K14+ progenitors involves combined KIT and FGFR2b signaling for proliferation and doubling of the cell number.

Expansion of Distal Progenitors Is Essential for Branching Morphogenesis

We then asked whether distal progenitor cell expansion is required for branching morphogenesis. We used two loss-of-function approaches: $Kit^{W/W}$ SMGs, which lack KIT signaling due to a SNP in the *W* locus (Chabot et al., 1988), and ISCK treatment of intact SMGs (Figures 5A–5H). In both E14 $Kit^{W/W}$ and ISCK-treated SMGs, we found a significant reduction in the number of cells expressing KIT, K14, SOX10, and p63 as determined by protein staining, FACS analysis, and mRNA expression (Figures 5A, 5B, 5E, S5A, and S5B). Importantly, loss of KIT signaling reduced branching in cultured ISCK-treated and E14 $Kit^{W/W}$ SMGs, which were smaller than $Kit^{W/+}$ and $Kit^{+/+}$ glands (Figures 5C, 5D, and S5C). Even though E14 $Kit^{W/W}$ SMGs were similar in size to E13 $Kit^{+/+}$ SMGs, they exhibited reduced branching in culture (Figures 5C, 5D, and S5C). Notably, this reduction in size was associated with differentiated ducts with limited proliferative capacity. Consequently, $Kit^{W/W}$ and ISCK-treated SMGs had reduced numbers of proximal K5+ progenitors and a concomitant increase in the number of K19+ duct cells (Figures 5A, 5B, and 5E). Increased expression of *Hbegf* and *Egfr* (Figure 5E), which drive ductal differentiation (Knox et al., 2010) and reduce proliferation, further supported this finding (Figures 5E and S5B). In sum, loss of KIT signaling drives ductal differentiation and reduces branching morphogenesis.

To confirm that the primary defect was due to loss of KIT function in the epithelium, and not in the mesenchyme or blood vessels, we cultured both $Kit^{W/W}$ and ISCK-treated wild-type epithelia. Both exhibited reduced growth compared with the $Kit^{+/+}$ and DMSO-treated controls (Figure 5F). As expected, they showed reduced staining for KIT, CCND1, and K14; increased staining for K19; and

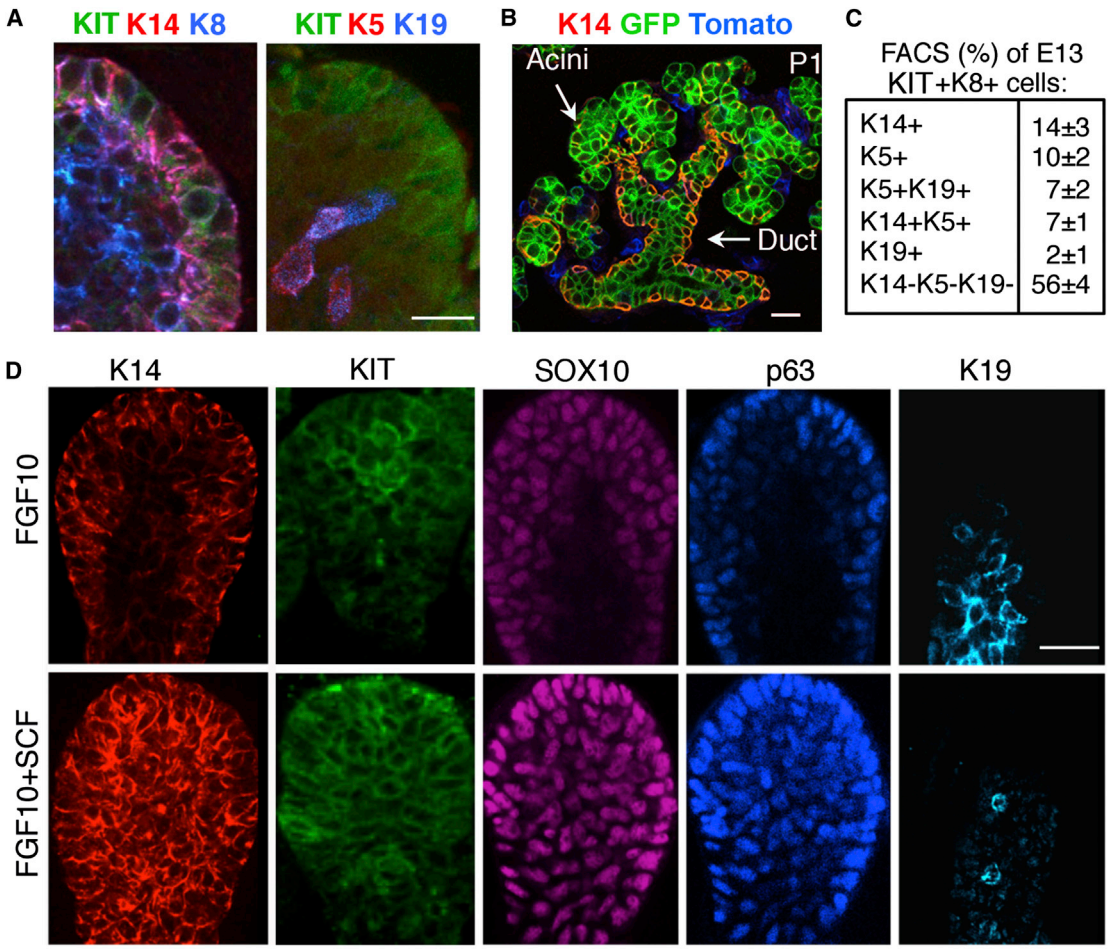

E

FACS (%) SMG cells:	FGF10	FGF10+ SCF
K14	**22**±2	**44**±3
KIT	**23**±1	**43**±2
SOX10	**11**±1	**20**±2
K19	42±4	42±2
ECAD	87±3	90±3
Ki67	8±1	9±1

F

FACS (%) KIT+K8+ cells:	FGF10	FGF10+ SCF
K14+	**3**±1	**8**±1
K14+K5+	**2**±1	**5**±1
K14+K19+	**8**±2	**13**±1
K14+K5+K19+	**16**±1	**33**±3
K14-K5+	3±1	1±2
K14-K5+K19+	23±3	14±2
K14-K19+	13±1	7±1
K14-K5-K19-	31±3	19±2

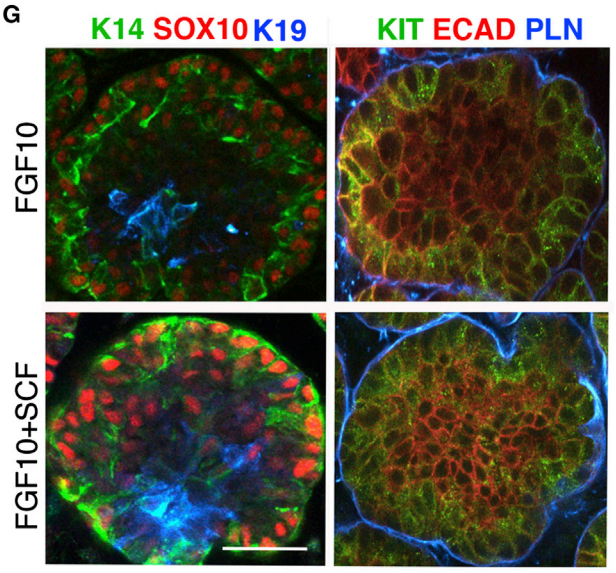

Figure 4. Combined KIT and FGFR2b Signaling Selectively Expands the Distal KIT+K14+SOX10+ Progenitors

(A) E13 endbud stained for KIT, K14, K8, K5, or K19. Pink cells coexpress K14 and K8 or K5 and K19. Images are 1 μm laser scanning confocal microscopy (LSCM) sections. Scale bar: 20 μm.

(legend continued on next page)

reduced expression of *Ccnd1*, *Sox10*, *Etv4*, *Etv5*, and *Myc* (Figures 5G and 5H). We conclude that reduced epithelial branching in $Kit^{W/W}$ and ISCK-treated glands was primarily due to reduced KIT signaling in the epithelium.

We further evaluated whether combined KIT and FGFR2b signaling has a conserved role in other organs that require FGFR2b, such as the lung. The lung, limb, kidney, liver, and pancreas express transcripts for *Kit* and *Kitl* (Figure S5D). At early stages (E10–E12), both lung epithelia and mesenchyme expressed *Kit* mRNA and protein as determined by qPCR, in situ analysis, and immunostaining (Figures S5E–S5G). Lung KIT+ cells are proliferative (CCND1+), express the progenitor marker SOX9 (Lu et al., 2008), and are located in FGFR2b+ and inhibitor of DNA binding 2 (ID2)+ endbuds (Rawlins et al., 2009). However, in E14 lung epithelia, KIT protein was not detectable and there was reduced *Kit* expression compared with earlier stages (Figures S5E and S5G). Similar to the case with SMGs, the loss of KIT signaling in E13 $Kit^{W/W}$ lungs resulted in ~40% smaller lungs, and there was reduced branching morphogenesis in E11 lungs cultured with ISCK for 48 hr (Figures S5H and S5I). This correlated with a reduction in expression of TFs (*Id2*, *Sox9*, *Myc*, *Etv4*, and *Etv5*) in lung endbuds (Figure S5J). Furthermore, there was reduced expression of proliferation (*Ccnd1*) and neuroendocrine cell markers (*Sv2b* and *Calca*), suggesting that KIT signaling may also impact these cell types. The primary defect in lung branching was also due to reduced KIT signaling in the epithelia, as shown by treating E10 lung epithelia with ISCK (Figure S5K). In gain-of function experiments with lung epithelia, SCF alone did not affect proliferation (Figure S5L), but altered TF gene expression when combined with FGF10. These data suggest that KIT and FGFR2b signaling expands progenitors by regulating a cassette of TFs in both SMGs and lungs.

Distal KIT+ Progenitors Communicate with the Neuronal Niche to Maintain Proximal Progenitors and Coordinate Ductal Architecture

Since a loss of KIT signaling depletes both distal and proximal progenitors, and proximal progenitors are maintained by innervation (Knox et al., 2010), we hypothesized that communication occurs between these distinct progenitors via the neuronal niche. To test this, we analyzed the parasympathetic innervation in $Kit^{W/W}$ and ISCK-treated SMGs. In both situations, we observed defects in epithelial innervation and reduced nerve function (Figure 6A). There was reduced defasciculation (arrowhead), such that fewer but wider nerve bundles extended toward the endbuds. Nerves also contained fewer varicosities (Figure 6A, middle panels), which release neurotransmitters such as acetylcholine. Loss of neuronal function in $Kit^{W/W}$ and ISCK-treated SMGs was confirmed by measuring reduced expression of *Tubb3* (an axonal marker), *Gfra2* (a parasympathetic marker), and markers of neuronal acetylcholine function (vesicular acetylcholine transporter [*Slc18a3* or *Vacht*] and choline acetyltransferase [*Chat*]; Figure 6B). Similar reductions of innervation and similar trends in the reduction of neuronal function were observed when KIT signaling was inhibited with ISCK at later stages of development after branching morphogenesis had occurred (Figures S6A and S6B). Washout of ISCK resulted in reinnervation, continued branching morphogenesis, and increased expression of genes associated with neuronal function (Figures S6B and S6C). These data suggest that maintenance of epithelial-neuronal communication requires KIT signaling.

To confirm that KIT signaling in KIT+ mesenchymal or endothelial cells did not influence nerve defasciculation and proximal K5+ progenitors, we recombined isolated epithelia from either Kit^{WW} or Kit^{WW};*K5*Venus mice with control ($Kit^{+/+}$) mesenchyme, which contains endothelial and neuronal cells. Recombined SMGs had reduced epithelial endbud growth and innervation (Figures 6C and S6D), and depletion of K5+ progenitors occurred in the Kit^{WW};*K5*Venus SMGs (Figure S6E) as compared with control. Taken together, these data confirm that KIT signaling in distal epithelial progenitors is essential for functional innervation and maintenance of proximal K5+ progenitors.

Since loss of KIT signaling affects K5+ proximal progenitors indirectly via the nerves, we predicted that we could rescue the K5+ cells from ISCK treatment with CCh and

(B) Lineage tracing of K14 in P1 SMG from a K14Cre x $Rosa^{mTmG}$ mouse. K14 progeny cells (GFP), endogenous K14 (red and yellow), and non-K14 cells (Tomato). Images are 2 μm LSCM sections. Scale bar, 20 μm.
(C) FACS analysis of K5, K14, and K19 cells in an epithelial KIT+K8+ cell population of E13 SMGs. Mean ± SEM; n > 3 biological samples.
(D) Staining of K14, KIT, SOX10, p63, and K19 in epithelia cultured for 24 hr in FGF10−/+ SCF. Scale bar, 20 μm.
(E) FACS analysis of KIT, K14, SOX10, K19, ECAD, and Ki67 in E13 SMGs cultured for 72 hr in FGF10−/+ SCF. Data are mean ± SEM; n > 3 biological samples.
(F) FACS analysis of K14-, K5-, and K19-expressing cells in the epithelial K8+KIT+ cell population in E13 SMGs cultured for 72 hr in FGF10−/+ SCF. Data are mean ± SEM; n = 3 biological samples.
(G) E13 SMGs cultured for 72 hr in FGF10−/+ SCF were stained for K14, SOX10, and K19, or KIT, ECAD, and Perlecan (PLN). Images are 1 μm LSCM sections. Scale bar, 20 μm.
See also Figure S4.

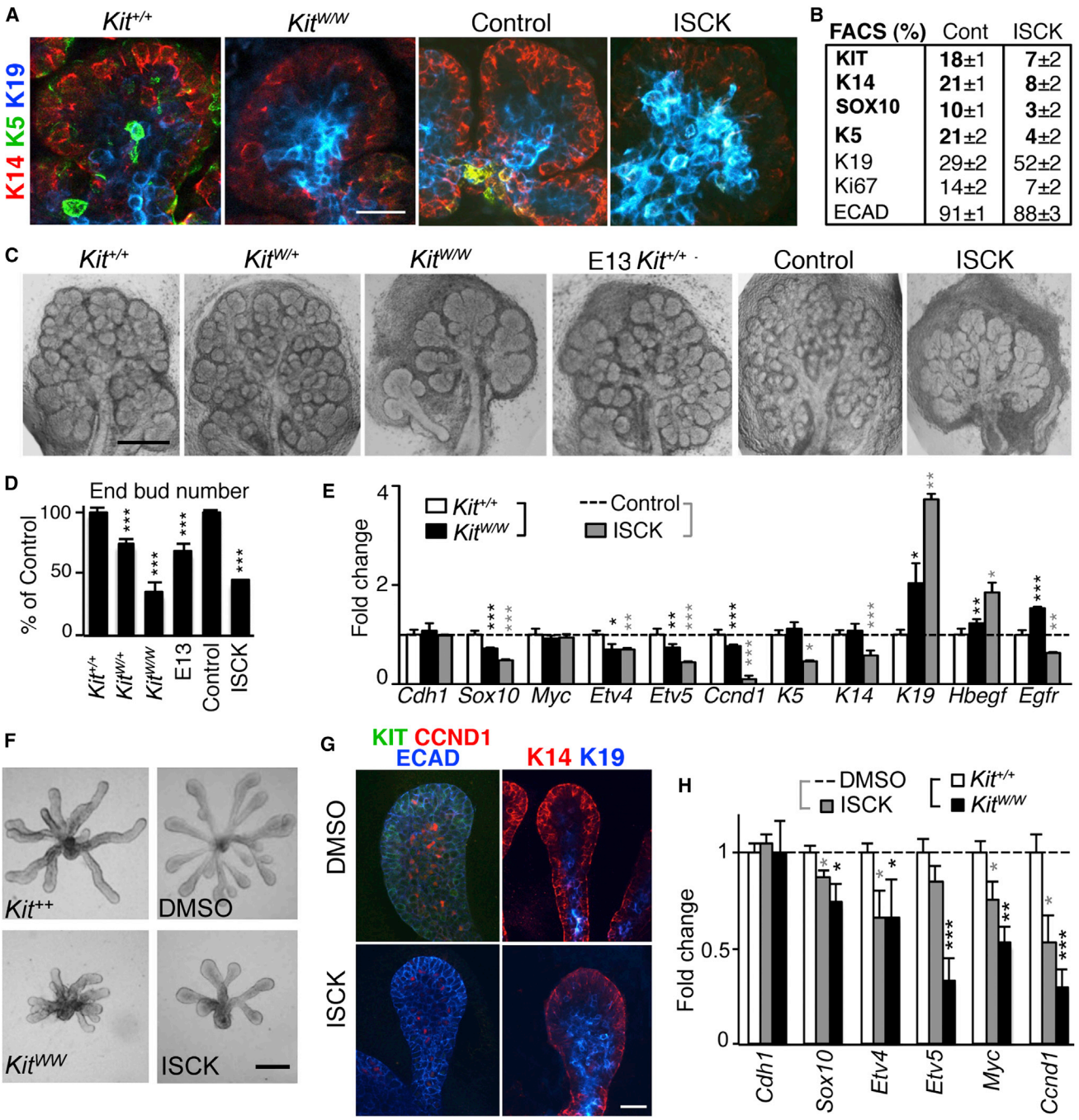

Figure 5. Loss of Epithelial KIT Signaling Reduces Branching Morphogenesis by Depleting Both K14+ and K5+ Progenitors

(A) Staining for K14, K5, and K19 in E14 SMG endbuds from *Kit*$^{+/+}$ and *Kit*$^{W/W}$ mice or E13 SMGs cultured for 72 hr with DMSO or ISCK. Images are 1 μm LSCM sections. Scale bar, 20 μm.

(B) FACS analysis of KIT, K14, SOX10, K5, K19, Ki67, and ECAD in E13 SMGs cultured with DMSO (Cont) or ISCK. Data are mean ± SEM; n > 3 biological samples.

(C) E14 and E13 SMGs from *Kit*$^{+/+}$, *Kit*$^{W/+}$, and *Kit*$^{W/W}$ embryos cultured for 24 hr, and E13 SMGs cultured in DMSO (Control) or ISCK for 72 hr. Scale bar, 200 μm.

(D) Endbud number from (C). Data are normalized to 0 hr and E14 *Kit*$^{+/+}$ or Control. Unpaired t test, ***p < 0.01, ISCK versus DMSO, *Kit*$^{W/+}$ and *Kit*$^{W/W}$ versus *Kit*$^{+/+}$, and E13 versus *Kit*$^{W/W}$. Unpaired t test, ***p < 0.01; n > 3 biological samples.

(legend continued on next page)

HBEGF, which maintain K5+ progenitors (Knox et al., 2010). The addition of CCh and HBEGF to ISCK-treated SMGs maintained K5+ cells, but K14+ proximal progenitors were not rescued (Figures 6D and S6F). There was also no increase in branching morphogenesis or expression of *Krt14*, *Kit*, and *Sox10* (Figure S6F). These data suggest that coordination of the organ's architecture requires KIT-mediated expansion of K14+ distal progenitors.

We then hypothesized that KIT+ cells secrete neurotrophic factors that promote innervation and neuronal function. We recently identified that neurturin (NRTN) is produced by SMG epithelium and is important for neuronal survival (Knox et al., 2013). $Kit^{W/W}$ and ISCK-treated SMGs showed reduced *Nrtn* expression compared with controls (Figure 6B). Furthermore, FACS-sorted epithelial KIT+FGFR2b+ cells from E13 SMGs had 3-fold more *Nrtn* expression than KIT− cells (Figure S6G). In addition, we confirmed that this occurred both in $Kit^{W/W}$ lungs and in control E11 lungs treated with ISCK, in which we also observed reduced innervation and varicosities (Figure S6H). Importantly, in both situations there was reduced *Nrtn*, *Tubb3*, and *Vacht* expression (Figure S6H). There was also reduced *Gfra2* in $Kit^{W/W}$ lungs and reduced *Chat* expression with ISCK treatment. Thus, the reduction in neuronal gene expression is likely secondary to the reduction in NRTN. We conclude that the production of neurotrophic factors by distal KIT+ progenitors is a conserved mechanism to support the neuronal niche during organogenesis.

KIT Signaling in a Rare Population of Adult KIT+FGFR2b+ Progenitors Maintains Epithelial-Neuronal Communication during Homeostasis

Since adult SMG epithelial KIT+ cells (Lombaert et al., 2008) and lung KIT+ cells (Kajstura et al., 2011) were used for regeneration, we sought to determine whether our findings from organogenesis were conserved during adult tissue homeostasis. Immunostaining of the adult SMG revealed that KIT+ cells were localized in intercalated ducts (IDs; Figure 7A), which harbor progenitor cells based on label-retaining assays (Man et al., 2001) and are in close proximity to differentiated Aquaporin5+ acinar cells (Figure 7B). Adult mouse lungs exhibited abundant KIT+Vimentin+ or KIT+CD31+ blood vessels, with only rare epithelial KIT+ECAD+ or K18+ cells detected (Figure S7A). Similar to what was observed during organogenesis, adult SMG KIT+ progenitors were proliferative (CCND1+) (Figures 7C and 7F) and expressed FGFR2b on their cell membrane (Figures 7D and 7F). To compare their expression with that of embryonic KIT+ cells, we FACS sorted adult SMG epithelial LIN-EPCAM+KIT+FGFR2b+ cells, termed KIT+FGFR2b+. FGFR2b was expressed on fewer KIT+ cells in the adult SMG (23% ± 3%, green peak; Figure 7E) compared with KIT+ cells in E13 SMGs (90% ± 4%, green peak; Figure 7E). Since KIT+ cells account for ~3% of epithelial cells in the adult gland (Lombaert et al., 2008), adult KIT+FGFR2b+ cells are a rare population of 0.6% ± 0.2%. Intriguingly, qPCR analysis of adult KIT+FGFR2b+ sorted cells revealed a striking similarity to embryonic KIT+ progenitors, with *Etv4*, *Sox10*, *Ccdn1*, and *Nrtn* being highly expressed compared with KIT+FGFR2b− cells (Figure 7F). Therefore, we predicted that KIT and FGFR2b signaling in adult ID epithelial cells might also maintain communication with nerves. Since $Kit^{W/W}$ is embryonic lethal, we cultured adult wild-type SMG explants for 3 days in the presence of ISCK. As predicted, neuronal innervation was affected (Figure 7G) and K5 and K14 staining was reduced along with an increase in ductal K19+ cells (Figure 7H). Accordingly, ISCK reduced expression of *Tubb3*, *Krt5*, *Krt14*, *Kit*, and *Ccnd1* (Figure 7J). Conversely, adding FGF10 and SCF increased cell proliferation and *Ccnd1* (Figures 7I and 7J). Taken together, these data indicate that during organ homeostasis, KIT signaling also maintains the ductal architecture via communication among multiple epithelial progenitors and their niches.

Finally, we confirmed that a similar KIT+FGFR2b+ cell population occurs in human salivary glands (Figure 7K). Human SMG KIT+ cells are located in IDs and excretory ducts (EDs). Although many KIT+ cells expressed SOX10 (Figure S7B), only a rare population of KIT+ cells coexpressed FGFR2 (Figure 7K). Surprisingly, we also detected KIT expression on acinar cells, which may make them potentially responsive to KIT signaling as well, although they were not FGFR2+. The working model presented in Figure 7L shows that mesenchymal-derived SCF and FGF10 expand KIT+FGFR2b+ distal progenitors that

(E) qPCR analysis of E14 $Kit^{+/+}$ and $Kit^{W/W}$ SMGs, and SMGs cultured for 72 hr with DMSO (Control) or ISCK. Data were normalized to E14 $Kit^{+/+}$ or Control (dotted line), respectively, and *Rps29*. Unpaired t test, *p < 0.05, **p < 0.01, ***p < 0.001; n = 3 biological samples.
(F) Isolated $Kit^{W/W}$ epithelia and E13 epithelia treated with ISCK for 48 hr undergo less epithelial morphogenesis than control epithelia. Scale bar, 20 μm.
(G) Isolated epithelia cultured with ISCK for 48 hr have reduced staining for KIT, CCND1, and K14, and increased K19 staining. LCSM image of 1 μm section through endbud.
(H) Gene-expression profile of $Kit^{+/+}$ and $Kit^{W/W}$ or DMSO and ISCK-treated epithelia. Data were normalized to control (DMSO or $Kit^{+/+}$) and *Rps29*. Unpaired t test, *p < 0.05, **p < 0.01, ***p < 0.001; n = 3 biological samples.
See also Figure S5.

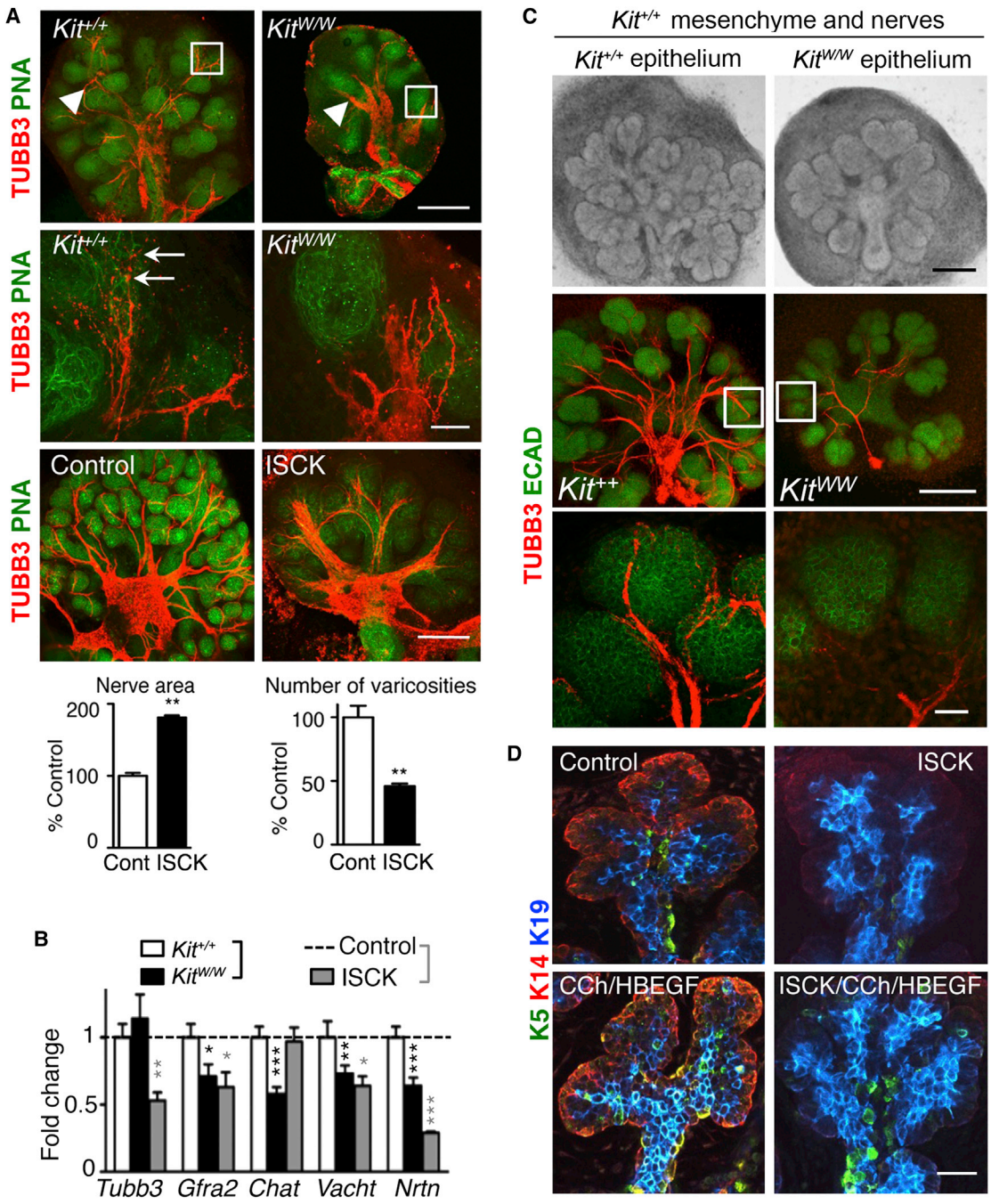

Figure 6. KIT Signaling in Distal Epithelial Progenitors Is Essential for Epithelial-Neuronal Communication and Maintenance of Proximal K5+ Progenitors

(A) Staining for nerves (TUBB3) and epithelium (PNA) in E14 *Kit*$^{+/+}$ and *Kit*$^{W/W}$ SMGs and E13 SMGs cultured for 72 hr with DMSO (Control) or ISCK. White box in upper panels is shown in middle panels. Arrowheads represent axons, arrows indicate varicosities. Scale bars, 200 μm (upper and lower panels) and 20 μm (middle panel). Images are 1 μm LSCM sections. Graphs show nerve area (area of nerves/area of epithelia) and varicosities (number of varicosities per area of TUBB3). Mean ± SEM. Unpaired t test, $^{**}p < 0.05$.

(B) qPCR analysis of genes that are markers of neuronal function in E14 *Kit*$^{+/+}$ and *Kit*$^{W/W}$ SMGs, and in E13 SMGs cultured for 72 hr with DMSO (Control) or ISCK. Data were normalized to Control (dotted line) or E14 *Kit*$^{+/+}$, respectively, and *Rps29*. Unpaired t test, $^{*}p < 0.05$, $^{**}p < 0.01$, $^{***}p < 0.001$; n = 3 biological samples.

(legend continued on next page)

coordinate organ architecture by establishing communication between multiple niches and proximal progenitors.

DISCUSSION

Here, we propose that combined KIT and FGFR2b signaling regulates epithelial progenitor expansion. We identify an interaction between KIT and FGFR2b signaling pathways that converges to upregulate a conserved group of FGFR2b-dependent TFs and expand distal progenitors. These progenitors further communicate with the neuronal niche to direct proximal progenitors to form ducts. These interactions are maintained during adult organ homeostasis, and exist in human organs. Our findings may have implications for regenerative medicine because they demonstrate that both KIT and FGFR2b signaling and communication among multiple cell types are necessary for organogenesis.

We propose that a similar conserved mechanism occurs in other organs, because FGFR2b signaling is required to initiate development of mammary, pituitary, and thyroid glands, as well as the kidney, pancreas, and prostate (Lin et al., 2007; Mailleux et al., 2002; Ohuchi et al., 2000). Similarly, KIT is expressed in these organs and is essential for kidney and prostate development (La Rosa et al., 2008; Leong et al., 2008; Li et al., 2007; Schmidt-Ott et al., 2006; Ulivi et al., 2004). Although previous studies have shown that FGFR2b signaling induces progenitor survival and proliferation (Bhushan et al., 2001; Ohuchi et al., 2000), we now demonstrate that it is a key upstream driver that induces distal KIT+ progenitor expansion. FGFR2b signaling achieves this by upregulating the KIT pathway to maintain KIT+-responsive progenitors. This is a critical event because combined KIT and FGFR2b signaling pathways converge at the transcriptional level to upregulate the expression of a conserved cassette of FGFR2b-dependent TFs in KIT+ progenitors. Distal progenitors of other organs, such as the pancreas (Kobberup et al., 2007) and limb (Zhang et al., 2009), express ETV4 and ETV5, which are part of this conserved TF cassette. Our experiments with L6 rat myoblasts also suggest that conserved TFs are upregulated when KIT and FGFR2b are overexpressed in cells where they are not normally present, and that for each cell type additional TFs may provide a cell-type-specific response.

We also propose that the KIT/FGFR2b pathway likely integrates with other signaling pathways to direct progenitor expansion. For example, WNT signaling has been proposed to be a master regulator of lung development (Rajagopal et al., 2008). Yet, our data suggest that WNT and KIT/FGFR2b can affect distal progenitors in different ways. The specific loss of WNT7b did not alter the number of *Sox9* or SOX9+ cells in lungs, whereas loss of KIT signaling reduced *Sox9* in lung endbuds. In contrast to WNT signaling, KIT does not directly influence CCND1-mediated proliferation, and although lung development is arrested in FGFR2b$^{-/-}$ mice, it is only reduced in β-Catenin$^{-/-}$ mice (Mucenski et al., 2003; Shu et al., 2005). It will be interesting to determine whether the neuronal niche is affected in WNT-depleted mice.

Prior to this work, we did not fully understand how epithelial progenitors communicate with their surrounding niche during organogenesis (Bryant and Mostov, 2008; Hogan, 1999). Here, we propose that a key mechanism is distal progenitor expansion, since these cells produce critical neurotrophic signals to communicate with the neuronal niche to regulate proximal progenitors. Neurturin is also produced by distal progenitors in the kidney (Davies et al., 1999) and is found in the prostate, pituitary gland, and pancreas (Golden et al., 1999). It is not known whether KIT+ cells secrete neurotrophic factors in these organs.

Previous studies have shown that paracrine and autocrine morphogenic gradients control branching morphogenesis, and a number of models propose the existence of iterative positive and negative unidirectional cues between the epithelium and mesenchyme or within the epithelial lineage (Bryant and Mostov, 2008; Gjorevski and Nelson, 2011; Hogan, 1999; Hsu and Fuchs, 2012). These studies provided valuable insights into organogenesis, but focused on communication from a single cell type. Progenitors in vivo must interpret signals from multiple cell types in their surrounding microenvironment during organogenesis. Our work has implications for regenerative medicine and the bioengineering of tissues, which may require multiple progenitor cell types to generate branching organs. Also, our findings will inform efforts to expand epithelial progenitors in vitro, which will be critical in clinical settings where small numbers of progenitors from biopsies could be expanded with reagents that target FGFR2b, KIT, and the neuronal niche. We propose that using progenitor

(C) Recombination of *Kit*$^{+/+}$ or *Kit*^{WW} epithelia with *Kit*$^{+/+}$ mesenchyme cultured for 72 hr shows that loss of epithelial KIT signaling reduces innervation. SMGs were stained for nerves (TUBB3) and ECAD. White box in upper panel is shown in lower panel. Scale bars, 200 and 20 μm, respectively.

(D) Staining of K5, K14, and K19 in endbuds from SMGs cultured with DMSO (Control), ISCK, and/or CCh and HBEGF. Images are 1 μm LCSM sections. Scale bar, 20 μm.

See also Figure S6.

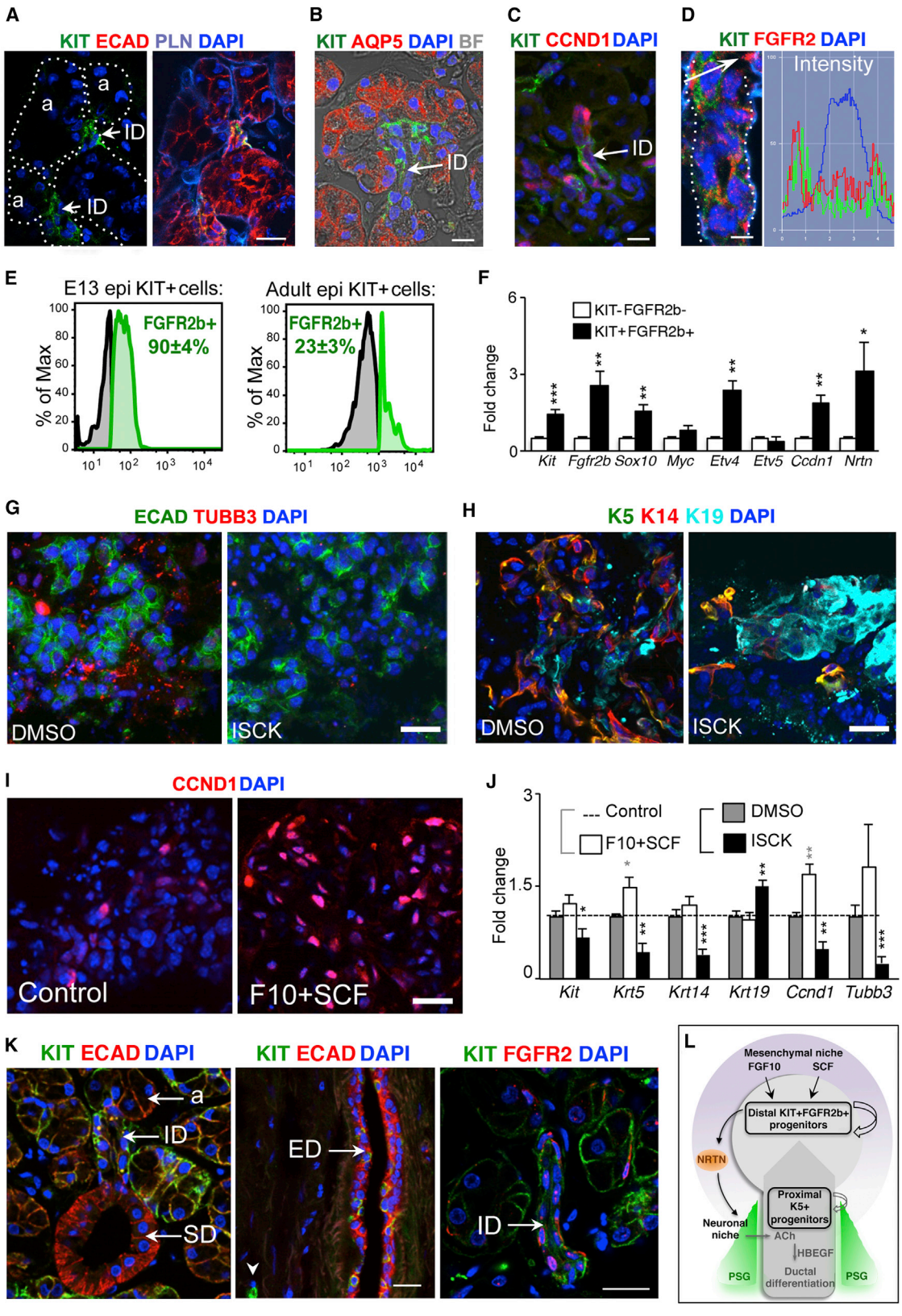

(legend on next page)

transplants with factors that preserve nerves will improve regeneration of damaged organs. For instance, nerves may facilitate the production of insulin (Rossi et al., 2005) after grafting of beta-progenitors to treat diabetic neuropathy and pancreatitis (Melton, 2011), or enhance lung repair after progenitor transplants (Rock and Hogan, 2011).

It has been proposed that tumors and organs are similar in terms of the complexity of cell types, microenvironments, and signaling networks involved in these components (Hanahan and Weinberg, 2011). The clonal nature of cancer means that targeting a single RTK may provide selective pressure for resistant tumor clones (Nik-Zainal et al., 2012). It is also possible that an activating KIT or FGFR2 mutation in an FGFR2b- or KIT-expressing tumor, respectively, may expand a dominant tumor clone and amplify downstream responses. Thus, by targeting KIT and FGFR2b, and/or the signals between the progenitors and their niches, we may be able to target tumors more efficiently. In conclusion, a clear resolution of the signaling pathways and communication among multiple cell types that are representative of the endogenous microenvironment during organogenesis and homeostasis provides insight into tumor biology and a framework to direct therapeutic organ regeneration.

EXPERIMENTAL PROCEDURES

Mouse Lines, Breeding, Genotyping, and Lineage Tracing

All protocols involving mice (Supplemental Experimental Procedures) were approved by the NIH ACUC. Culture of Mo7e and L6 cells, and staining of human biopsies are described in the Supplemental Experimental Procedures.

Ex Vivo Organ Culture

We performed fetal and adult intact organ and mesenchyme-free epithelia culture of SMG or lung in the presence of different growth factors and/or inhibitors as described in the Supplemental Experimental Procedures.

qPCR

Real-time qPCR was performed as previously described (Knox et al., 2013). cDNAs were generated and amplified to determine fold changes in expression by normalizing to the housekeeping gene *Rps29*. The generation of single amplicon products was confirmed by melt curve analysis.

Immunofluorescence Analysis and FACS

We performed whole-mount immunofluorescence as described in the Supplemental Experimental Procedures. For FACS, single-cell suspensions of SMGs were analyzed on either a BD Calibur or an LSRII, and sorted on a BD Aria sorter (see Supplemental Experimental Procedures). Negative cell populations were used as controls.

In Situ Hybridization

Digoxigen-11-UTP-labeled single-stranded RNA probes were prepared using the DIG RNA labeling kit (Roche Applied Science) according to the manufacturer's instructions.

Western Blot Analysis

Protein lysates were resolved on Tris gels, transferred to membranes, probed with antibodies, and visualized with West Dura reagent as described in detail in the Supplemental Experimental Procedures.

Statistical Analysis

Experiments were performed with at least three biological replicates. To determine significance between two groups, comparisons were made using Student's t test. Analysis of multiple groups was

Figure 7. KIT Signaling Regulates Epithelial-Neuronal Communication during Homeostasis in a Rare Population of Adult KIT+FGFR2b+ Cells that Are Present in Human SMGs

(A–D) Staining of KIT, ECAD, PLN, Aquaporin 5 (AQP5), CCND1, FGFR2b, and DAPI in adult mouse SMGs. Arrows indicate IDs near acinar cells (a). Scale bar, 10 μm. Graph represents the protein intensity of KIT and FGFR2b through an ID cell. BF, bright field.

(E) Histogram of FACS analysis showing the total number of FGFR2b+ cells within the epithelial (EPCAM+, epi) KIT+ population in E13 and adult SMGs. Data are mean ± SEM; n > 3 biological samples. Gray area, KIT+FGFR2b− cells; green area, KIT+FGFR2b+ cells.

(F) qPCR analysis of FACS-sorted adult SMG epithelial LIN-EPCAM+KIT+FGFR2b+ and LIN-EPCAM+KIT-FGFR2b− cells. Data were normalized to KIT-FGFR2b− cells and *Rps29*. Unpaired t test, *p < 0.05, **p < 0.01; n = 3 biological samples.

(G and H) Adult SMG explants cultured for 3 days with ISCK. Staining of ECAD, nerves (TUBB3), and DAPI in (G), and K14, K19, K5 and DAPI in (H). Images are 10 μm LCSM sections. Scale bars: 20 μm.

(I) Adult SMG explants cultured for 3 days ± FGF10+SCF were stained for CCND1 and DAPI. Images are 1 μm LSCM section. Scale bar, 20 μm.

(J) qPCR analysis of adult SMG explants cultured in basal media (Control), FGF10+SCF, DMSO, or ISCK for 72 hr. Data were normalized to Control or DMSO, and *Rps29*. Unpaired t test, *p < 0.05, **p < 0.01, ***p < 0.001; n = 3 biological samples.

(K) Staining of KIT, ECAD, DAPI, and FGFR2 in human SMGs. Images are 1 μm LSCM section. Scale bars, 20 μm. a, acinar cells; SD, striated duct.

(L) Working model. Multicellular communication initiated by combined KIT and FGFR2b signaling establishes the branching architecture during organogenesis and adult homeostasis.

See also Figure S7.

performed by one-way ANOVA. For statistical tests, $p < 0.05$ was considered statistically significant.

SUPPLEMENTAL INFORMATION

Supplemental Information includes Supplemental Experimental Procedures and seven figures and can be found with this article online at http://dx.doi.org/10.1016/j.stemcr.2013.10.013.

ACKNOWLEDGMENTS

We thank Dr. P. McCoy and Dr. A. Williams from the NHLBI Flow Cytometry Core for technical support, Dr H. Ye (YU) for technical assistance with the L6 cells, Dr. S. Pradhan Bhatt (UD) for assistance with human samples, and Dr. S. Gutkind (NIDCR) and Dr. G. Martin (UCSF) for providing the K14Cre and Rosa^{mTmG} reporter mice. I.M.A.L. received a Dutch Niels Stensen Stichting Award for young Dutch academics to gain experience abroad. This study was supported by the Intramural Research Program of the National Institute of Dental and Craniofacial Research, NIH, DHHS.

Received: September 4, 2013
Revised: October 30, 2013
Accepted: October 31, 2013
Published: December 12, 2013

REFERENCES

Bhushan, A., Itoh, N., Kato, S., Thiery, J.P., Czernichow, P., Bellusci, S., and Scharfmann, R. (2001). Fgf10 is essential for maintaining the proliferative capacity of epithelial progenitor cells during early pancreatic organogenesis. Development *128*, 5109–5117.

Bryant, D.M., and Mostov, K.E. (2008). From cells to organs: building polarized tissue. Nat. Rev. Mol. Cell Biol. *9*, 887–901.

Casaletto, J.B., and McClatchey, A.I. (2012). Spatial regulation of receptor tyrosine kinases in development and cancer. Nat. Rev. Cancer *12*, 387–400.

Chabot, B., Stephenson, D.A., Chapman, V.M., Besmer, P., and Bernstein, A. (1988). The proto-oncogene c-kit encoding a transmembrane tyrosine kinase receptor maps to the mouse W locus. Nature *335*, 88–89.

Davies, J.A., Millar, C.B., Johnson, E.M., Jr., and Milbrandt, J. (1999). Neurturin: an autocrine regulator of renal collecting duct development. Dev. Genet. *24*, 284–292.

De Moerlooze, L., Spencer-Dene, B., Revest, J.M., Hajihosseini, M., Rosewell, I., and Dickson, C. (2000). An important role for the IIIb isoform of fibroblast growth factor receptor 2 (FGFR2) in mesenchymal-epithelial signalling during mouse organogenesis. Development *127*, 483–492.

Gjorevski, N., and Nelson, C.M. (2011). Integrated morphodynamic signalling of the mammary gland. Nat. Rev. Mol. Cell Biol. *12*, 581–593.

Golden, J.P., DeMaro, J.A., Osborne, P.A., Milbrandt, J., and Johnson, E.M., Jr. (1999). Expression of neurturin, GDNF, and GDNF family-receptor mRNA in the developing and mature mouse. Exp. Neurol. *158*, 504–528.

Hanahan, D., and Weinberg, R.A. (2011). Hallmarks of cancer: the next generation. Cell *144*, 646–674.

Hogan, B.L. (1999). Morphogenesis. Cell *96*, 225–233.

Hsu, Y.C., and Fuchs, E. (2012). A family business: stem cell progeny join the niche to regulate homeostasis. Nat. Rev. Mol. Cell Biol. *13*, 103–114.

Jahn, T., Sindhu, S., Gooch, S., Seipel, P., Lavori, P., Leifheit, E., and Weinberg, K. (2007). Direct interaction between Kit and the interleukin-7 receptor. Blood *110*, 1840–1847.

Kajstura, J., Rota, M., Hall, S.R., Hosoda, T., D'Amario, D., Sanada, F., Zheng, H., Ogórek, B., Rondon-Clavo, C., Ferreira-Martins, J., et al. (2011). Evidence for human lung stem cells. N. Engl. J. Med. *364*, 1795–1806.

Kent, D., Copley, M., Benz, C., Dykstra, B., Bowie, M., and Eaves, C. (2008). Regulation of hematopoietic stem cells by the steel factor/KIT signaling pathway. Clin. Cancer Res. *14*, 1926–1930.

Kiger, A.A., White-Cooper, H., and Fuller, M.T. (2000). Somatic support cells restrict germline stem cell self-renewal and promote differentiation. Nature *407*, 750–754.

Knox, S.M., Lombaert, I.M., Reed, X., Vitale-Cross, L., Gutkind, J.S., and Hoffman, M.P. (2010). Parasympathetic innervation maintains epithelial progenitor cells during salivary organogenesis. Science *329*, 1645–1647.

Knox, S.M., Lombaert, I.M., Haddox, C.L., Abrams, S.R., Cotrim, A., Wilson, A.J., and Hoffman, M.P. (2013). Parasympathetic stimulation improves epithelial organ regeneration. Nat. Commun. *4*, 1494.

Kobberup, S., Nyeng, P., Juhl, K., Hutton, J., and Jensen, J. (2007). ETS-family genes in pancreatic development. Dev. Dyn. *236*, 3100–3110.

La Rosa, S., Uccella, S., Dainese, L., Marchet, S., Placidi, C., Vigetti, D., and Capella, C. (2008). Characterization of c-kit (CD117) expression in human normal pituitary cells and pituitary adenomas. Endocr. Pathol. *19*, 104–111.

Lemmon, M.A., and Schlessinger, J. (2010). Cell signaling by receptor tyrosine kinases. Cell *141*, 1117–1134.

Leong, K.G., Wang, B.E., Johnson, L., and Gao, W.Q. (2008). Generation of a prostate from a single adult stem cell. Nature *456*, 804–808.

Li, J., Quirt, J., Do, H.Q., Lyte, K., Fellows, F., Goodyer, C.G., and Wang, R. (2007). Expression of c-Kit receptor tyrosine kinase and effect on beta-cell development in the human fetal pancreas. Am. J. Physiol. Endocrinol. Metab. *293*, E475–E483.

Lin, Y., Liu, G., Zhang, Y., Hu, Y.P., Yu, K., Lin, C., McKeehan, K., Xuan, J.W., Ornitz, D.M., Shen, M.M., et al. (2007). Fibroblast growth factor receptor 2 tyrosine kinase is required for prostatic morphogenesis and the acquisition of strict androgen dependency for adult tissue homeostasis. Development *134*, 723–734.

Lombaert, I.M., Brunsting, J.F., Wierenga, P.K., Faber, H., Stokman, M.A., Kok, T., Visser, W.H., Kampinga, H.H., de Haan, G., and Coppes, R.P. (2008). Rescue of salivary gland function after stem cell transplantation in irradiated glands. PLoS ONE *3*, e2063.

Lombaert, I.M., Knox, S.M., and Hoffman, M.P. (2011). Salivary gland progenitor cell biology provides a rationale for therapeutic salivary gland regeneration. Oral Dis. *17*, 445–449.

Lu, Y., Okubo, T., Rawlins, E., and Hogan, B.L. (2008). Epithelial progenitor cells of the embryonic lung and the role of microRNAs in their proliferation. Proc. Am. Thorac. Soc. *5*, 300–304.

Mailleux, A.A., Spencer-Dene, B., Dillon, C., Ndiaye, D., Savona-Baron, C., Itoh, N., Kato, S., Dickson, C., Thiery, J.P., and Bellusci, S. (2002). Role of FGF10/FGFR2b signaling during mammary gland development in the mouse embryo. Development *129*, 53–60.

Man, Y.G., Ball, W.D., Marchetti, L., and Hand, A.R. (2001). Contributions of intercalated duct cells to the normal parenchyma of submandibular glands of adult rats. Anat. Rec. *263*, 202–214.

Melton, D.A. (2011). Using stem cells to study and possibly treat type 1 diabetes. Philos. Trans. R. Soc. Lond. B Biol. Sci. *366*, 2307–2311.

Mucenski, M.L., Wert, S.E., Nation, J.M., Loudy, D.E., Huelsken, J., Birchmeier, W., Morrisey, E.E., and Whitsett, J.A. (2003). beta-Catenin is required for specification of proximal/distal cell fate during lung morphogenesis. J. Biol. Chem. *278*, 40231–40238.

Nanduri, L.S., Lombaert, I.M., van der Zwaag, M., Faber, H., Brunsting, J.F., van Os, R.P., and Coppes, R.P. (2013). Salisphere derived c-Kit(+) cell transplantation restores tissue homeostasis in irradiated salivary gland. Radiother. Oncol. *13*, 240–245.

Nik-Zainal, S., Van Loo, P., Wedge, D.C., Alexandrov, L.B., Greenman, C.D., Lau, K.W., Raine, K., Jones, D., Marshall, J., Ramakrishna, M., et al.; Breast Cancer Working Group of the International Cancer Genome Consortium (2012). The life history of 21 breast cancers. Cell *149*, 994–1007.

Ohuchi, H., Hori, Y., Yamasaki, M., Harada, H., Sekine, K., Kato, S., and Itoh, N. (2000). FGF10 acts as a major ligand for FGF receptor 2 IIIb in mouse multi-organ development. Biochem. Biophys. Res. Commun. *277*, 643–649.

Rajagopal, J., Carroll, T.J., Guseh, J.S., Bores, S.A., Blank, L.J., Anderson, W.J., Yu, J., Zhou, Q., McMahon, A.P., and Melton, D.A. (2008). Wnt7b stimulates embryonic lung growth by coordinately increasing the replication of epithelium and mesenchyme. Development *135*, 1625–1634.

Rawlins, E.L., Clark, C.P., Xue, Y., and Hogan, B.L. (2009). The Id2+ distal tip lung epithelium contains individual multipotent embryonic progenitor cells. Development *136*, 3741–3745.

Rock, J.R., and Hogan, B.L. (2011). Epithelial progenitor cells in lung development, maintenance, repair, and disease. Annu. Rev. Cell Dev. Biol. *27*, 493–512.

Rock, J.R., Onaitis, M.W., Rawlins, E.L., Lu, Y., Clark, C.P., Xue, Y., Randell, S.H., and Hogan, B.L. (2009). Basal cells as stem cells of the mouse trachea and human airway epithelium. Proc. Natl. Acad. Sci. USA *106*, 12771–12775.

Rossi, J., Santamäki, P., Airaksinen, M.S., and Herzig, K.H. (2005). Parasympathetic innervation and function of endocrine pancreas requires the glial cell line-derived factor family receptor alpha2 (GFRalpha2). Diabetes *54*, 1324–1330.

Schmidt-Ott, K.M., Chen, X., Paragas, N., Levinson, R.S., Mendelsohn, C.L., and Barasch, J. (2006). c-kit delineates a distinct domain of progenitors in the developing kidney. Dev. Biol. *299*, 238–249.

Shen, Q., Goderie, S.K., Jin, L., Karanth, N., Sun, Y., Abramova, N., Vincent, P., Pumiglia, K., and Temple, S. (2004). Endothelial cells stimulate self-renewal and expand neurogenesis of neural stem cells. Science *304*, 1338–1340.

Shu, W., Guttentag, S., Wang, Z., Andl, T., Ballard, P., Lu, M.M., Piccolo, S., Birchmeier, W., Whitsett, J.A., Millar, S.E., and Morrisey, E.E. (2005). Wnt/beta-catenin signaling acts upstream of N-myc, BMP4, and FGF signaling to regulate proximal-distal patterning in the lung. Dev. Biol. *283*, 226–239.

Takeuchi, K., and Ito, F. (2011). Receptor tyrosine kinases and targeted cancer therapeutics. Biol. Pharm. Bull. *34*, 1774–1780.

Ulivi, P., Zoli, W., Medri, L., Amadori, D., Saragoni, L., Barbanti, F., Calistri, D., and Silvestrini, R. (2004). c-kit and SCF expression in normal and tumor breast tissue. Breast Cancer Res. Treat. *83*, 33–42.

Wagers, A.J. (2012). The stem cell niche in regenerative medicine. Cell Stem Cell *10*, 362–369.

Wu, H., Klingmüller, U., Besmer, P., and Lodish, H.F. (1995). Interaction of the erythropoietin and stem-cell-factor receptors. Nature *377*, 242–246.

Zhang, Z., Verheyden, J.M., Hassell, J.A., and Sun, X. (2009). FGF-regulated Etv genes are essential for repressing Shh expression in mouse limb buds. Dev. Cell *16*, 607–613.